Nonlinear photoacoustic spectroscopy of hemoglobin

Amos Danielli, Konstantin Maslov, Christopher P. Favazza, Jun Xia, and Lihong V. Wang

Citation: Applied Physics Letters **106**, 203701 (2015); doi: 10.1063/1.4921474
View online: http://dx.doi.org/10.1063/1.4921474
View Table of Contents: http://scitation.aip.org/content/aip/journal/apl/106/20?ver=pdfcov
Published by the AIP Publishing

Nonlinear photoacoustic spectroscopy of hemoglobin

Amos Danielli,[a] Konstantin Maslov, Christopher P. Favazza, Jun Xia, and Lihong V. Wang[b]
Optical Imaging Laboratory, Department of Biomedical Engineering, Washington University in St. Louis, One Brookings Drive, St. Louis, Missouri 63130, USA

(Received 19 March 2015; accepted 11 May 2015; published online 18 May 2015)

As light intensity increases in photoacoustic imaging, the saturation of optical absorption and the temperature dependence of the thermal expansion coefficient result in a measurable nonlinear dependence of the photoacoustic (PA) signal on the excitation pulse fluence. Here, under controlled conditions, we investigate the intensity-dependent photoacoustic signals from oxygenated and deoxygenated hemoglobin at varied optical wavelengths and molecular concentrations. The wavelength and concentration dependencies of the nonlinear PA spectrum are found to be significantly greater in oxygenated hemoglobin than in deoxygenated hemoglobin. These effects are further influenced by the hemoglobin concentration. These nonlinear phenomena provide insights into applications of photoacoustics, such as measurements of average inter-molecular distances on a nm scale or with a tuned selection of wavelengths, a more accurate quantitative PA tomography.
 [http://dx.doi.org/10.1063/1.4921474]

Photoacoustic microscopy (PAM) is an effective *in vivo* functional and molecular imaging tool. In the PA phenomenon, light is absorbed by molecules and converted to heat. Subsequent thermoelastic expansion generates an acoustic wave, termed the PA wave.[1,2] Detection of PA waves sequentially excited at multiple optical wavelengths provides quantitative information about the concentrations of multiple chromophores such as oxygenated and deoxygenated hemoglobin molecules in red blood cells. Thus, the relative concentration and the oxygen saturation (sO_2) of hemoglobin can be extracted.[3–5] Generally, the amplitude of the PA signal is assumed to be linearly proportional to the excitation pulse fluence. However, as the excitation laser intensity increases, both the saturation of the optical absorption[6,7] and the temperature dependence of thermal expansion[8–10] result in a measurable nonlinear dependence of the PA signal on the excitation pulse fluence. PA nonlinearity has recently been used in several applications such as quantifying picosecond absorption relaxation times with a nanosecond laser,[6] differentiating optical absorbers,[10] measuring oxygen saturation *in vivo*,[7] and performing label-free PA nanoscopy of biological structures having undetectable fluorescence.[11] In the presence of nonlinearity, quantitative PA measurements require a detailed analysis of the intensity-dependence of the PA signal, particularly for hemoglobin, the major intrinsic absorber in tissue for PA imaging. Based on thermal nonlinearity, analysis of the nonlinear PA signal from a single point source has been previously discussed.[8] However, the wavelength- and concentration-dependent effects of both optical saturation and thermal nonlinearity on the PA signals for multiple absorbers have not been reported. Here, we investigate nonlinear PA effects in oxygenated and deoxygenated hemoglobin using a PA spectrometer with a flat-top beam illumination, which effectively reduces uncertainty in our measurements that would otherwise arise from inhomogeneous spatial distribution of the optical fluence. In oxygenated whole blood, we show that the wavelength dependence of the nonlinear PA spectrum is significantly greater than in deoxygenated whole blood. Moreover, we show how the nonlinear PA spectrum of oxygenated lysed blood is affected by different concentrations of hemoglobin molecules.

Nonlinear PA effects arise from two major sources: nonlinear thermal expansion and optical absorption saturation. First, the thermal expansion coefficient, $\beta(T)$, depends on the temperature rise T above the equilibrium temperature, T_0. When T is small, $\beta(T) \approx \beta_1 + \beta_2 T$, where β_1 and β_2 are the first two coefficients in the Taylor expansion around T_0. In the sample used in our system, the average inter particle distance (on the nm scale) is several orders of magnitude smaller than the acoustic wavelength, Λ (e.g., 49 μm for a 30 MHz transducer). Hence, the sample can be considered as acoustically homogenous. In addition, the laser pulse duration (~5 ns) is sufficiently shorter than the transducer response time (several tens of nanoseconds), and therefore, the photoacoustic excitation is in stress confinement within the acoustically defined resolution. In stress confinement, the initial volume-averaged temporal pressure rise, p_0, centered at $\vec{r}_0 = 0$ within the acoustic voxel V, is approximated by[8,12]

$$p_0 \approx \frac{1}{V_0 \kappa} \int_V \left[\beta_1 T(\vec{r}) + \frac{1}{2} \beta_2 (T(\vec{r}))^2 \right] \cdot d\vec{r}, \qquad (1)$$

where κ is the isothermal compressibility and V_0 is a volume of size smaller than the acoustic wavelength but much larger than the distance between of absorbers.

The second major source of nonlinear PA effects is saturation of the optical absorption coefficient with increasing light intensity.[13] For flat-top beam illumination, whose intensity is constant in the lateral direction, the optical absorption coefficient of a homogenous sample within the laser beam can be expressed as a function of depth z and time t

[a]Present address: Bar Ilan University, Faculty of Engineering, Ramat Gan 5290002, Israel.
[b]E-mail: LHWANG@WUSTL.EDU. Tel.: (314) 935-6152.

$$\mu_a(z,t) \cong \frac{\mu_{a0}}{1 + I(z,t)/\mathrm{I_{sat}}}. \quad (2)$$

Here, $\mu_{a0} = \sigma \cdot N$ is the unsaturated optical absorption coefficient (m^{-1}), σ is the absorption cross section, N is the number of absorbers per unit volume, $I(z,t)$ is the intensity of the light beam at depth z at time t, and $I_{sat} = h\nu/\tau_r\sigma$ is the saturation intensity of the absorbing molecule, where τ_r is the absorption relaxation time, h is the Planck's constant, and ν is the frequency.

Following Beer's Law, in the presence of optical absorption, the optical intensity attenuates with depth, z. However, when the transducer's bandwidth is sufficiently large, so that the characteristic acoustic wavelength, Λ (e.g., 49 μm) is smaller than the penetration depth (e.g., in our experiment, for oxygenated bovine hemoglobin at 11.5 g/dl concentration, $1/\mu_{a0} \cong 73\,\mu$m at 532 nm, and the scattering effect is negligible), Beer's Law attenuation has a negligible effect on the detected peak PA amplitude.[14] Thus, at the sample surface, within the acoustic voxel, the intensity is approximated as time-varying only. In other words, $I(z,t) \approx I(0,t)$, and consequently, according to Eq. (2), the absorption coefficient becomes $\mu_a(z,t) \approx \mu_a(0,t)$.

To calculate the effects of thermal nonlinearity and optical saturation on the PA signal, we considered the optical illumination in our experiments. The optical intensity at $z = 0$ was presumed to have the following general form:

$$I(z=0,\vec{r},t) = E_p \hat{f}_s(\vec{r}) \hat{f}_t(t). \quad (3)$$

Here, E_p is the pulse energy and $\hat{f}_s(\vec{r})$ is the normalized spatial function. For a flat-top beam illumination, $\hat{f}_s(\vec{r}) = \frac{1}{\pi R^2}\mathrm{rect}(\frac{\vec{r}}{2R})$, where R is the beam radius and $rect(\cdot)$ is a rectangular function. $\hat{f}_t(t)$ is the normalized temporal function. For a Gaussian pulse, $\hat{f}_t(t) = \frac{1}{\sqrt{2\pi}\tau_L}\exp[-\frac{t^2}{2\tau_L^2}]$, where τ_L is a parameter related to the FWHM of the pulse (FWHM $= 2\sqrt{2\ln(2)}\tau_L$). For a beam radius much larger than the acoustic wavelength, the intensity is considered to be constant in the lateral direction and $I(z=0,\vec{r},t)$ is reduced to $I(z=0,t)$.

For weak saturation (i.e., $I(z=0,t) \ll \mathrm{I_{sat}}$), the optical energy deposition ($\mathrm{J/m^3}$) at the sample surface due to single photon absorption can be expanded in Taylor's series as

$$A_e = \int_{-\infty}^{\infty} \mu_a(0,t) I(0,t) \cdot dt \approx \mu_{a0} I_{sat} \int_{-\infty}^{\infty} (\hat{I} - \hat{I}^2 + \hat{I}^3 \cdots + (-1)^{n-1} \cdot \hat{I}^n)\mathrm{dt}, \quad (4)$$

where $\hat{I} = I(t)/\mathrm{I_{sat}}$. For an incident beam with a Gaussian pulse, Eq. (4) becomes

$$A_e \approx \mu_{a0} F_{\mathrm{sat}} \left(\sqrt{\frac{1}{1}}\hat{F} - \sqrt{\frac{1}{2}}\hat{F}^2 + \sqrt{\frac{1}{3}}\hat{F}^3 \cdots + (-1)^{n-1}\sqrt{\frac{1}{n}}\hat{F}^n \right), \quad (5)$$

where $F_{\mathrm{sat}} = \sqrt{2\pi}\tau_L I_{\mathrm{sat}}$ and $\hat{F}$ is the incident fluence normalized by F_{sat}, $\hat{F} = F/F_{\mathrm{sat}}$.

To evaluate the effect of thermal nonlinearity and optical saturation, we need to look at two different cases, namely, densely packed and loosely packed absorbers (Fig. 1(a)). In densely packed molecules, the thermal diffusion length,[12] $d_{th} = \sqrt{\chi\tau_L}$, where χ is the thermal diffusivity, is small compared to the dimensions of the acoustically and optically defined voxel, and large compared to the distance between absorbing molecules. Hence, the photoacoustic excitation is in macroscopic but not microscopic thermal confinement. Consequently, the absorbing area can be approximated by a continuous medium with a smooth temperature distribution, and the local temperature rise, T, is given by

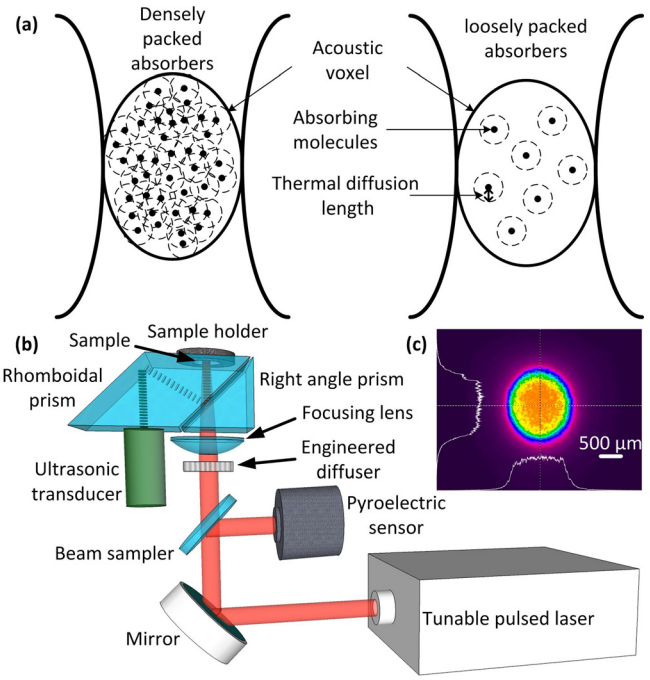

FIG. 1. (a) Densely and loosely packed absorbers within the acoustic voxel. (b) A photoacoustic spectrometer with flat-top beam illumination. (c) 2D beam profile.

$$T = \eta_{\mathrm{th}} A_e/(\rho C_p), \quad (6)$$

where η_{th} is the percentage of deposited optical energy that is converted into heat, ρ denotes the mass density, and C_p denotes the specific heat capacity at constant pressure. Thus, substituting Eqs. (6) and (5) into Eq. (1) yields

$$p_0(F) = c_1 \cdot F + c_2 \cdot F^2 + \cdots. \quad (7)$$

Here, the linear coefficient is $c_1 = \Gamma\eta_{th}\mu_{a0}$, where Γ is the Grueneisen coefficient. For a flat-top spatial intensity profile and densely packed absorbers, the second-order coefficient as a function of the wavelength, λ (referred to here as the nonlinear PA spectrum), becomes[11]

$$c_2(\lambda) = \sigma^2(\lambda)\left(-\Gamma_1\eta_{th}\frac{N\tau_r(\lambda)}{h\nu\sqrt{2\pi}\tau_L(\lambda)} + \Gamma_2\eta_{th}^2 N^2 \right), \quad (8)$$

where, Γ_1 and Γ_2 are constants proportional to β_1 and β_2, respectively. The wavelength-dependent effects of thermal nonlinearity and optical saturation can be evaluated after the second-order coefficient, $c_2(\lambda)$, is scaled by dividing by the square of the absorption cross section, $\sigma^2(\lambda)$. The first term in $c_2(\lambda)/\sigma^2(\lambda)$ is negative and related to optical saturation. It

is proportional to the absorption relaxation time of the molecule, $\tau_r(\lambda)$, and inversely proportional to the laser pulse width, $\tau_L(\lambda)$. Both parameters are wavelength-dependent. The second term in the $c_2(\lambda)/\sigma^2(\lambda)$ is positive, related to the thermal nonlinearity, constant at all wavelengths, and proportional to N^2.

For loosely packed molecules, the thermal diffusion length, d_{th}, is small compared to the distance between absorbing molecules (Fig. 1(a)). Hence, the photoacoustic excitation is in both macroscopic and microscopic thermal confinement. While the influence of optical saturation in the acoustic volume is the same, the contribution of thermal nonlinearity to the nonlinear PA signal is different. The heat distribution around each absorbing molecule is not affected by presence of other molecules. Hence, the thermal nonlinearity term in Eq. (8) is proportional to N rather than to N^2.

When the optical saturation term in Eq. (8) is negligible, the power, x, of the concentration, N^x, in the thermal nonlinearity term can be estimated by taking measurements of the second-order coefficient (c_2^a and c_2^b) at two different concentrations, N_a and N_b

$$x \cong \log\left(\frac{c_2^a}{c_2^b}\right) \Big/ \log\left(\frac{N_a}{N_b}\right). \tag{9}$$

To extract the linear and second-order coefficients in Eq. (7), we measured the PA spectrum as a function of the incident laser fluence, using a custom-built PA spectrometer (see Fig. 1(b)). A Q-Switched Nd:YAG laser (Quantel, Inc.) with 3rd harmonic (355 nm) output pumps an OPO laser (BasiScan, Newport), which works at 10 Hz in the wavelength range of 410–1050 nm. In the wavelength range of interest (500–600 nm), the laser's pulse width (τ_{FWHM}) varies linearly from 4.0 to 5.5 ns. The ultrasonic and optic coupling cube is made of a BK7 glass prism joined with a rhomboidal prism, with a layer of index-matching liquid between them. A sealed stainless steel sample cell with 10 mm inner diameter is attached to the rhomboidal prism. One milliliter of oxygenated or deoxygenated blood is deposited into the cell. The blood is temperature controlled and constantly stirred by a motor placed on top of the sample holder (not shown in Fig. 1(a)). An engineered diffuser (PRC Photonics) provides a flat-top beam profile with 5%–10% uniformity within a 1.24 mm optical beam diameter at the sample cell surface (see Fig. 1(b)). The photoacoustically generated ultrasonic signal is detected by an attached 30 MHz ultrasonic transducer (V213-BC-RM, Olympus). To measure the laser pulse energy, a small portion of the light is reflected to a pyroelectric detector (SPH-11, Spectrum Detector, Inc.), which is calibrated for a wide range of laser pulse energies (0.1–10.0 mJ) over the entire wavelength range (500–600 nm). The signals from the ultrasonic transducer and the pyroelectric detector are digitized using a 14 bit, 200 MHz digitizer (14200, Gage). To measure the PA spectrum, at each wavelength we

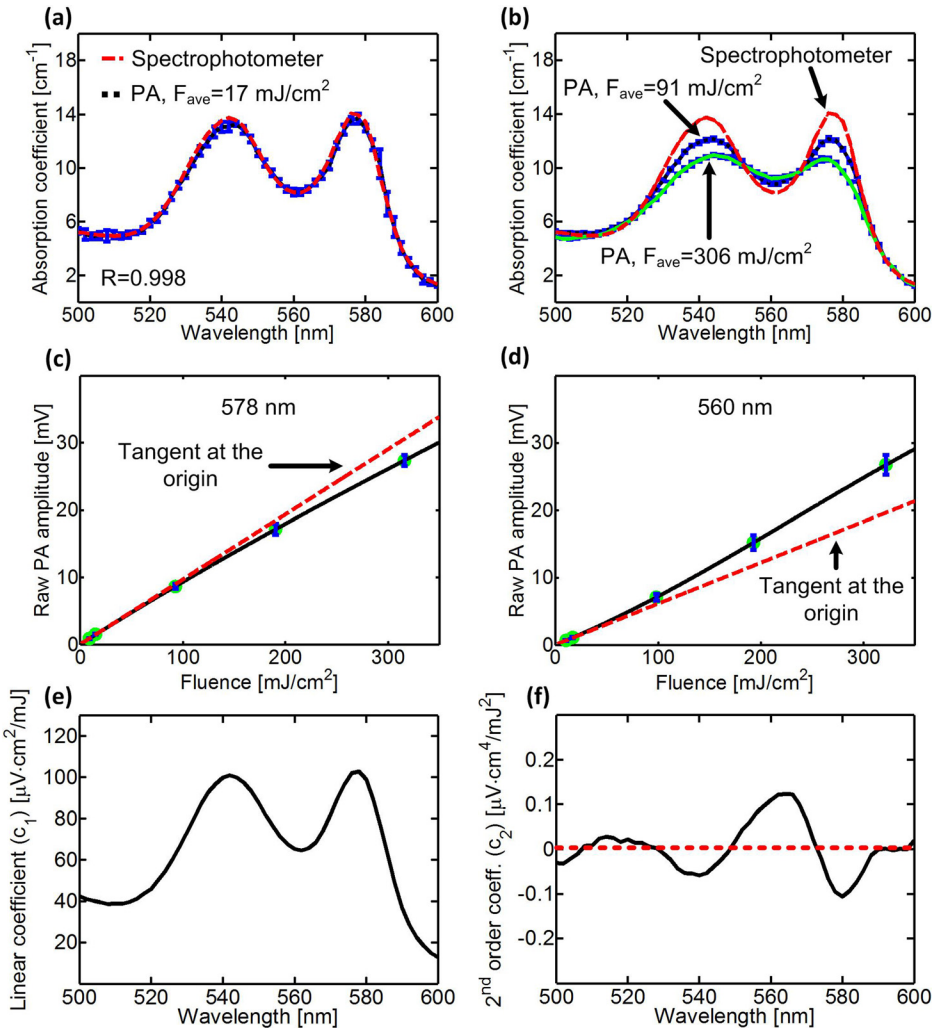

FIG. 2. (a) and (b) PA amplitude versus laser wavelength in fully oxygenated lysed blood (0.07 mM) at (a) low incident fluence and (b) high incident fluence. The red dashed line is the absorption spectrum, which fits the theoretical absorption of 98% oxygenated hemoglobin, measured by a spectrophotometer (Cary-50, Agilent). (c) and (d) PA amplitude as a function of the incident fluence at (c) 578 nm and (d) 560 nm. Each red dashed line is the tangent of the nonlinear curve at the origin. Error bars represent the standard deviations of ten measurements. (e) and (f) A typical (e) linear coefficient, c_1, and (f) 2nd order coefficient, c_2, as a function of the laser wavelength. The red dashed line represents $c_2 = 0$.

averaged the peak-to-peak amplitude of the PA signal generated from the sample surface by ten consecutive laser excitation pulses. The PA spectrum was taken for different average incident laser fluence values, ranging from 3 to 330 mJ/cm^2. The linear and second-order coefficients at each wavelength were extracted by fitting the averaged peak-to-peak amplitude of the PA signal from the sample surface as a function of the incident fluence to a 3rd order polynomial. Different concentrations of oxygenated lysed blood were prepared by mixing 2 ml of deionized water with different volumes (20 μl to 1280 μl) of oxygenated whole bovine blood (910–500, Quad Five). Deoxygenated whole blood was prepared by mixing bovine blood in a rotating flask with carbon dioxide for 4 h at 37 °C.

To first validate the linearity of our PA measurements at low average incident fluence (e.g., 17 mJ/cm^2), we compared the absorption spectrum of oxygenated lysed blood (0.07 mM of tetramer hemoglobin) measured by the PA spectrometer and a spectrophotometer (Cary-50, Agilent). For low PA laser excitation fluences, the correlation between the absorption spectra was high (R = 0.998), and the sO_2 was calculated to be 98% (Fig. 2(a)). As we increased the incident fluence, the PA spectrum deviated from the conventional absorption spectrum (Fig. 2(b)). At the absorption peaks of oxygenated hemoglobin (540 nm and 578 nm), the PA signal dropped as much as 26% below its expected value (Fig. 2(c)), and at other wavelengths (e.g., 560 nm), it rose as much as 13% above its expected value (Fig. 2(d)). The extracted linear coefficient (Fig. 2(e)) was proportional to the absorption spectrum with a correlation coefficient of 0.997. However, the extracted second-order coefficient (Fig. 2(f)) had strong wavelength dependence, with negative values around the absorption peaks of oxygenated hemoglobin, where optical saturation dominates, and positive values around 560 nm, where thermal nonlinearity dominates.

The conventional and nonlinear PA spectra of whole blood are presented in Figs. 3(a)–3(d). At low incident laser fluence, the measured PA spectrum correlated well with the theoretical absorption spectrum of deoxygenated whole blood (R = 0.999) with $sO_2 = 8\%$ (Fig. 3(a)). A typical second-order coefficient of deoxygenated lysed blood is shown in Fig. 3(b). To analyze the wavelength-dependent effects of optical saturation and thermal nonlinearity, we scaled the nonlinear PA spectra of deoxygenated and oxygenated whole blood by dividing by the square of their corresponding absorption cross sections (Figs. 3(c) and 3(d)). For deoxygenated hemoglobin, the absorption relaxation time is short.[6,7] Thus, optical saturation (the first term in Eq. (8)) is

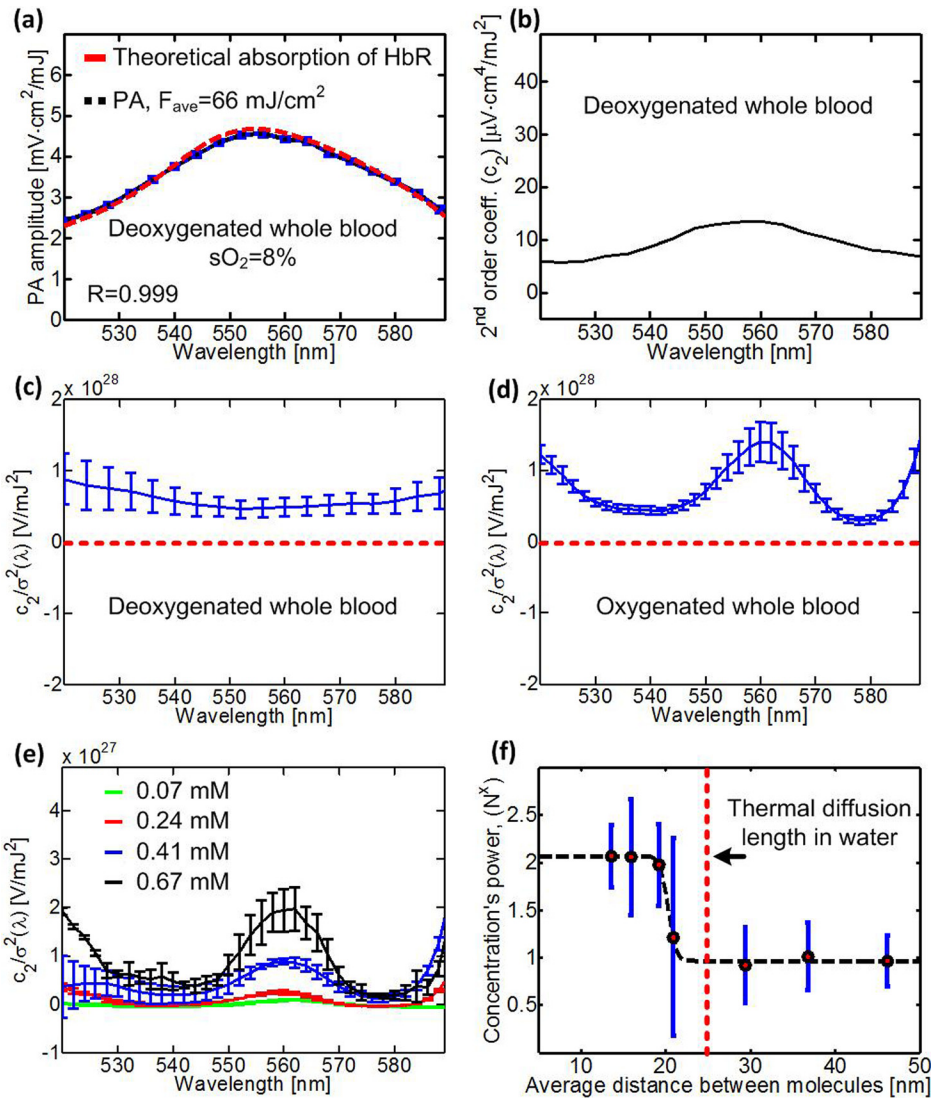

FIG. 3. (a) Photoacoustic amplitude versus laser wavelength in deoxygenated whole blood. (b) 2nd order coefficient, c_2, versus laser wavelength for deoxygenated whole blood. (c)–(e) $c_2/\sigma^2(\lambda)$ versus laser wavelength for (c) deoxygenated whole blood, (d) oxygenated whole blood, and (e) different concentrations of oxygenated lysed blood. The red dashed line represents $c_2 = 0$. (f) The concentration's power dependence of c_2 at 560 nm as a function of average distance between molecules. The red dashed line represents the thermal diffusion length (26 nm) in water for a 4.9 ns laser pulse width. Error bars in (a) represent the standard deviations of ten measurements. Error bars in (c)–(f) represent the standard errors of 3–4 experiments.

negligible, and the scaled second-order coefficient (Fig. 3(c)) is mostly constant in wavelength, with a relatively slight drop (25%) around the absorption peak of deoxygenated whole blood at 560 nm. In oxygenated whole blood, the absorption relaxation time is much longer, particularly at the absorption peaks around 540 nm and 578 nm. Therefore, the scaled second-order coefficient of oxygenated whole blood (Fig. 3(d)) has strong wavelength dependence, with minima at 540 nm and 578 nm. The positive peak at 560 nm suggests that for oxygenated hemoglobin, optical saturation at 560 nm is negligible, and thermal nonlinearity dominates.

To evaluate the concentration dependence of the nonlinear PA spectrum of oxygenated lysed blood, we extracted the scaled second-order coefficient at different concentrations (Fig. 3(e)). At high concentrations, the increase in the scaled second-order coefficient can clearly be seen, particularly at 560 nm, where thermal nonlinearity dominates. The power of the concentration as a function of the average distance between molecules is presented in Fig. 3(f). For oxyhemoglobin at 560 nm, optical saturation is negligible, and the 2nd order coefficient depends mostly on thermal nonlinearity. Thus, when the distance between the hemoglobin molecules is larger than the thermal diffusion length, c_2 at 560 nm is proportional to N. When the distance between the hemoglobin molecules is much smaller than the thermal diffusion length, c_2 at 560 nm is proportional to N^2.

In conclusion, using a custom-built PA spectrometer, we measured the intensity dependence of PA signals from oxygenated and deoxygenated hemoglobin at varied wavelengths, and extracted the nonlinear PA spectrum. For hemoglobin, the nonlinear PA spectrum has strong wavelength dependence. In particular, for oxygenated hemoglobin, the relatively long absorption relaxation time results in low saturation intensity, and therefore, the PA signal drops as much as 26% below its expected value at sufficiently high excitation intensities. This optical saturation effect dominates mostly around the absorption peaks at 540 nm and 578 nm. Previously, Steinke and Shepherd reported[15] that the absorption coefficient of oxygenated hemoglobin linearly drops with increasing temperature at 587 nm illumination. Specifically, for a temperature rise of 20 °C, the absorption coefficient decreased by 4%. The temperature rise in our experiments (e.g., for 0.07 mM of oxygenated hemoglobin, Fig. 2(b)) is ~200 mK, which according to the work of Steinke and Shepard could account for a maximum change of 0.04% in the hemoglobin absorption coefficient. In addition, we show that the amount of thermal nonlinearity generated in the excitation volume is affected by the average distance between absorbing molecules, r, relative to the thermal diffusion length, d_{th}. Thus, for shorter laser pulses, the thermal diffusion length decreases, and the contribution of the absorbers' concentration to the thermal nonlinearity term vanishes. This opens possibilities for measuring concentration of absorbing molecules in solution. Overall, understanding of these nonlinear phenomena provides insights into existing and future applications of photoacoustics.[6,7,9,11] For example, careful selection of wavelengths and laser pulse durations can improve the accuracy of quantitative functional PAM by minimizing nonlinear effects. In other applications, one might desire to maximize the nonlinear effects.

This work was sponsored in part by National Institutes of Health grants DP1 EB016986 (NIH Director's Pioneer Award), R01 CA186567 (NIH Director's Transformative Research Award), and R01 CA159959.

[1]A. A. Oraevsky, S. L. Jacques, and F. K. Tittel, "Measurement of tissue optical properties by time-resolved detection of laser-induced transient stress," Appl. Opt. **36**(1), 402–415 (1997).
[2]L. V. Wang and S. Hu, "Photoacoustic tomography: *In vivo* imaging from organelles to organs," Science **335**(6075), 1458–1462 (2012).
[3]X. D. Wang, X. Y. Xie, G. N. Ku, and L. H. V. Wang, "Noninvasive imaging of hemoglobin concentration and oxygenation in the rat brain using high-resolution photoacoustic tomography," J. Biomed. Opt. **11**(2), 024015 (2006).
[4]J. Laufer, D. Delpy, C. Elwell, and P. Beard, "Quantitative spatially resolved measurement of tissue chromophore concentrations using photoacoustic spectroscopy: Application to the measurement of blood oxygenation and haemoglobin concentration," Phys. Med. Biol. **52**(1), 141–168 (2007).
[5]H. F. Zhang, K. Maslov, G. Stoica, and L. H. V. Wang, "Functional photoacoustic microscopy for high-resolution and noninvasive *in vivo* imaging," Nat. Biotechnol. **24**(7), 848–851 (2006).
[6]A. Danielli, C. P. Favazza, K. Maslov, and L. V. Wang, "Picosecond absorption relaxation measured with nanosecond laser photoacoustics," Appl. Phys. Lett. **97**(16), 163701 (2010).
[7]A. Danielli, C. P. Favazza, K. Maslov, and L. H. V. Wang, "Single-wavelength functional photoacoustic microscopy in biological tissue," Opt. Lett. **36**(5), 769–771 (2011).
[8]I. G. Calasso, W. Craig, and G. J. Diebold, "Photoacoustic point source," Phys. Rev. Lett. **86**(16), 3550–3553 (2001).
[9]V. P. Zharov, "Ultrasharp nonlinear photothermal and photoacoustic resonances and holes beyond the spectral limit," Nat. Photonics **5**(2), 110–116 (2011).
[10]O. Simandoux, A. Prost, J. Gateau, and E. Bossy, "Influence of nanoscale temperature rises on photoacoustic generation: Discrimination between optical absorbers based on thermal nonlinearity at high frequency," Photoacoustics **3**(1), 20–25 (2015).
[11]A. Danielli, K. Maslov, A. Garcia-Uribe, A. M. Winkler, C. Y. Li, L. D. Wang, Y. Chen, G. W. Dorn, and L. V. Wang, "Label-free photoacoustic nanoscopy," J. Biomed. Opt. **19**(8), 086006 (2014).
[12]L. V. Wang and H.-I. Wu, *Biomedical Optics: Principles and Imaging* (Wiley-Interscience, Hoboken, New Jersey, 2007).
[13]A. E. Siegman, *Lasers* (University Science Books, Mill Valley, California, 1986).
[14]M. Sivaramakrishnan, K. Maslov, H. F. Zhang, G. Stoica, and L. V. Wang, "Limitations of quantitative photoacoustic measurements of blood oxygenation in small vessels," Phys. Med. Biol. **52**(5), 1349–1361 (2007).
[15]J. M. Steinke and A. P. Shepherd, "Effects of temperature on optical absorbance spectra of oxy-, carboxy-, and deoxyhemoglobin," Clin. Chem. **38**(7), 1360–1364 (1992); available at http://www.clinchem.org/content/38/7/1360.full.pdf.